

## Arbitrary-width confined states of traveling-wave convection: Pinning, locking, drift, and stability

Paul Kolodner

*AT&T Bell Laboratories, Murray Hill, New Jersey 07974-0636*

(Received 29 June 1993)

I describe observations of “arbitrary-width” confined states of traveling-wave convection in an ethanol-water mixture with separation ratio  $\psi = -0.253$ , made in an extremely uniform annular cell. The time derivative of the spatial width of these confined states vanishes at a unique, width-dependent Rayleigh number, not over a finite band of Rayleigh numbers as previously reported. Also, the confined states drift slowly around the cell, *backwards*.

PACS number(s): 47.27.Te, 47.20.Ky

Rayleigh-Bénard convection in a thin, horizontal layer of a binary-fluid mixture which is heated from below takes the form of traveling waves (TW's), which are triggered by a subcritical bifurcation from the quiescent state when the Rayleigh number  $r$  is increased above a threshold  $r_{co}$  [1,2]. Once nonlinear TW's fill the experimental cell, they will persist below onset, giving way to the quiescent state again only when  $r$  is reduced below a saddle-node Rayleigh number  $r_s < r_{co}$ . In the hysteresis loop between  $r_s$  and  $r_{co}$ , both TW's and the quiescent state are stable solutions of the equations of motion for this system. In the context of the complex Ginzburg-Landau equation (CGLE), a frequently used model of this system, it is possible for these two states to stably coexist, separated in space by fronts, if the system is sufficiently large [3]. This model also has “pulse” solutions; i.e., narrow convective structures surrounded by inactive fluid [3]. In this paper, I refer generally to such localized convecting regions surrounded by quiescent fluid as “confined states.”

The first confined state of TW's observed in this system was created in a narrow, rectangular cell [4], and was subsequently shown to closely resemble a pulse solution of a subcritical CGLE [3,5]. Experimentally, TW pulses have been studied at separation ratios  $\psi$  in the range  $-0.13 \lesssim \psi \lesssim -0.03$ . Their spatial structure—in particular, their width—is remarkably insensitive to experimental parameters, and they drift slowly through a sufficiently uniform cell [5–7]. The drift velocity  $v_{dr}$  is extremely sensitive to the local Rayleigh number. For most experimental parameters, pulses drift forwards; i.e., in the same direction as the phase velocity of the underlying TW's [6]. Many important features of fixed-width TW pulses have been reproduced in numerical integrations of the full Navier-Stokes equations in two dimensions [8]. While the slow drift cannot be properly modeled using a single-field CGLE, Riecke has recently shown how to self-consistently derive a CGLE coupled to a slow mean concentration field; this coupling causes pulses to drift at slow velocities that are qualitatively consistent with experimental observations [9].

For more negative separation ratios, confined-state behavior in this system is quite different. In experiments at  $\psi = -0.25$  reported in Ref. [10], confined states of any

width could be created. Once such an “arbitrary-width” confined state was made, its spatial extent could be made time independent by changing the Rayleigh number  $r$  to a value inside a narrow band (width 2.3% in [10]) deep inside the hysteresis loop. The confined state could be made to grow (shrink) only by adjusting  $r$  above (below) this Rayleigh-number band. Remarkably, inside this “locking band,” the width of the confined state remained fixed, and there was no spatial drift, even if  $r$  was moved around inside the band.

Many of the experimental features of arbitrary-width confined states were also observed in the numerical simulations of the authors of Ref. [8]. For  $\psi = -0.25$ , they observed a wide confined state whose frequency and spatial structure matched experimental observations in detail [11]. Wide confined states were also observed in the coupled-field model of Ref. [9], for the case of a CGLE with purely real coefficients. Wide confined states drift forwards in Ref. [8] and backwards in Ref. [9], in contradiction to each other and to the experimental observations. A much more serious puzzle, however, is presented by the observation of a continuum of confined-state widths for each Rayleigh number in the locking band, because confined-state solutions of the single-field CGLE are known to form a countable, discrete set [3]. Locking cannot arise in this model, even if “nonadiabatic” effects are included [12].

These discrepancies, along with an advancing understanding of the experimental role of inhomogeneities [6,13], have raised the suspicion that the locking band and the lack of drift seen in Refs. [10,11] were experimental artifacts, caused by pinning of the confined-state boundaries by imperfections in the experimental cell. To resolve these issues, I have conducted new experiments on arbitrary-width confined states in the cell with greatly improved spatial uniformity [6,13]. I find that these confined states drift *backwards*. More importantly, while there is a hint of “locking” in the raw data, this quickly disappears when the data are corrected by subtracting off a smooth function of confined-state width. To within quite high precision, there is no “locking band.”

The apparatus and techniques used in these experiments have been extensively described in recent publications [6,13]. The cell is an annular channel of height

$d = 0.2737$  cm, radial width  $1.677d$ , and mean circumference  $82.47d$ , formed by a concentric plastic disk and ring which are clamped between an electrically heated, mirror-polished silicon bottom plate and a transparent, water-cooled sapphire top plate. The fractional spatial uniformity and temporal stability of the applied vertical temperature difference are  $4 \times 10^{-4}$  and  $5 \times 10^{-5}$ , respectively. The flow pattern is viewed from above by a shadowgraphic flow-visualization system and is recorded by an annular array of 720 photodiodes. In the present experiments, this pattern consists of radial wave fronts which propagate around the cell in a single azimuthal direction under a spatially localized amplitude profile. This profile and the corresponding wave-number profile are extracted from the raw signal by demodulation in space at the measured mean wave number, using the techniques described in Ref. [13]. The precision of these calculations is at the 1% level. The fluid is an 8 wt % solution of ethanol in water at a mean temperature of  $27.8^\circ\text{C}$ , for which the separation ratio  $\psi = -0.253$ , Prandtl number  $P = 8.93$ , and the Lewis number  $L = 0.0079$  [14]. In this paper, lengths are scaled by the cell height  $d$ , and velocities are scaled by  $d/\tau_v$ , where  $\tau_v = 55.6$  sec is the vertical thermal diffusion time. The sign of velocities is defined by the direction of TW propagation.

TW convection is triggered in this system at  $r_{co} = 1.45974(18)$  and persists down to  $r_s = 1.2421(8)$  [15]. Inside this hysteresis loop, confined states can be created using techniques described in Refs. [6,10]. I have studied confined states at Rayleigh numbers in the range  $1.328 \lesssim r \lesssim 1.349$ . Most of the confined states studied had spatial widths in the range  $8 < w < 12$ , with a few data points taken at much larger widths. All of the confined states studied were narrower than half the circumference of the cell. A typical example of a wide

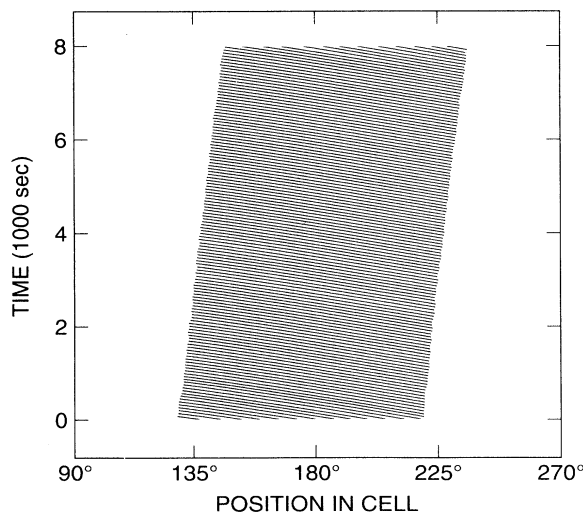


FIG. 1. Space-time paths of the convective roll boundaries are shown for a confined state of spatial width 21.1. The reduced Rayleigh number for this run was  $r = 1.3402$ . Rolls propagate to the left at a velocity  $v_{ph} = 1.480$ , while the confined state as a whole drifts to the right at a velocity  $v_{dr} = -0.0237$ .

confined state is shown in Fig. 1. This state exhibited a full width at half maximum spatial width of 21.1, and its amplitude and wave-number profiles match the measurements presented in Ref. [11]. The TW's in this state propagate to the left with phase velocity  $v_{ph} = 1.480$ , while the amplitude profile drifts in the opposite direction at a much lower velocity:  $v_{dr} = -0.0237$ . I have allowed confined states like this one to drift around the cell continually for weeks, taking approximately 60 h ( $4000\tau_v$ ) for a round trip.

Quantitative measurements of the drift and the spatial growth of arbitrary-width confined states are presented in Fig. 2. To produce each data point in these graphs, a confined state was allowed to evolve for several hours at constant Rayleigh number, and then a series of flow-visualization images was recorded over the next several hours. The leading- and trailing-edge fronts of the confined state were identified at each time step as the 50% points in the demodulated TW amplitude profile. Differentiating in time to produce the front velocities  $v_l$  and  $v_t$ , respectively, I define the drift velocity  $v_{dr} = (v_l + v_t)/2$  and the expansion velocity  $\Delta v = v_l - v_t$ . As shown in Fig. 2(a), the drift velocity depends very little on the Rayleigh number or on the confined-state width. The weighted average of the data points in Fig. 2(a) is  $\bar{v}_{dr} = -0.0205(34)$ . The expansion velocity, plotted in Fig. 2(b), increases with Rayleigh number, with a slope of about 3. The data exhibit substantial scatter; a fit to a cubic polynomial in  $r$  exhibits an rms residual of 0.0033. It might be thought at first that the slight flattening of the trend of the data seen in the range  $1.335 \lesssim r \lesssim 1.340$  represents a locking band obscured by the scatter. However, both of these features are caused in fact not by locking but by the dependence of the expan-

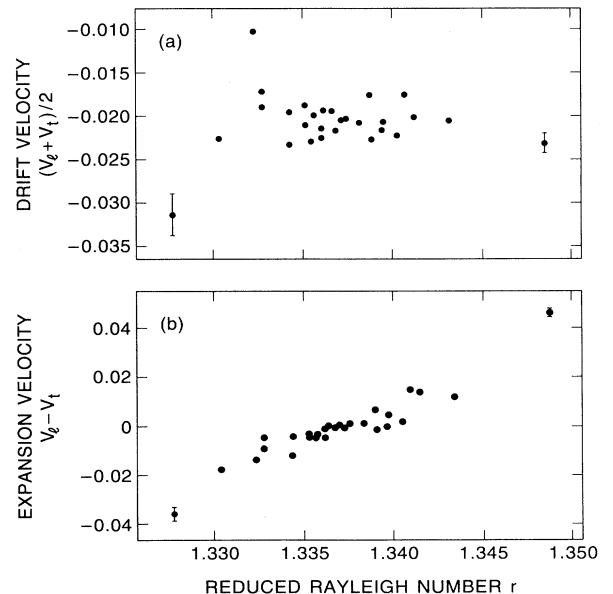


FIG. 2. Mean drift velocity  $v_{dr} = (v_l + v_t)/2$  (a) and the expansion velocity  $\Delta v = v_l - v_t$  (b) are plotted as functions of the reduced Rayleigh number  $r$ . In this and subsequent figures, error bars are shown when larger than the symbol.

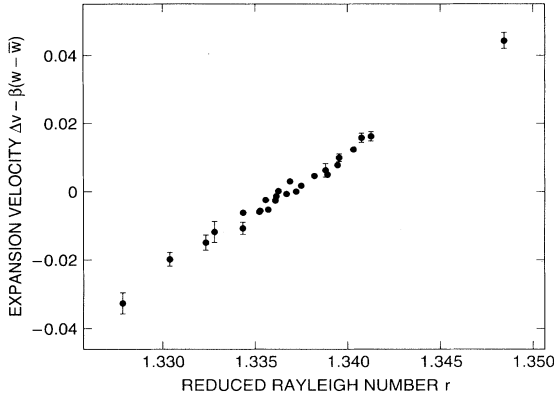


FIG. 3. Width-corrected expansion velocity  $\Delta\bar{v} = \Delta v - \beta(w - \bar{w})$  is plotted as a function of the reduced Rayleigh number  $r$ . To within the experimental precision,  $\Delta\bar{v}$  is a smooth function of  $r$  with a unique intercept  $r_v = 1.33648(23)$ .

sion of the confined state on its width  $w$ . I extracted this dependence by fitting the data points  $\Delta v(r, w)$  to the sum of a cubic in  $r$  and a linear function  $\beta(w - \bar{w})$ , where  $\bar{w} = 10$  is the average experimental width. Using the fit parameter  $\beta$ , the width dependence of  $\Delta v(r, w)$  can be removed by computing  $\Delta\bar{v}(r) = \Delta v(r, w) - \beta(w - \bar{w})$  for each data point. This width-corrected expansion velocity is plotted vs Rayleigh number in Fig. 3. The error bars in this graph are somewhat larger than those in Fig. 2(b) because the confined-state width  $w$  is not constant in time during most of the measurements; this introduces uncertainty in the width correction  $\beta(w - \bar{w})$ . Nonetheless, the width correction has reduced the scatter in the data to 0.0015 rms and has revealed a smooth dependence of  $\Delta\bar{v}$  on  $r$ . The fitted function of  $r$  passes through the horizontal axis with slope  $\tau_o^{-1} = 3.27(20)$  at an intercept  $r_v = 1.33648(23)$ , which I interpret as the unique value at which a confined state of width  $\bar{w}$  neither grows nor shrinks. To within this very high precision, there is no locking band.

To the extent that the width-corrected expansion velocity is linear in the Rayleigh number, confined-state evolution can be represented by a simple differential equation:

$$\tau_o \frac{dw}{dt} = r - r_o(w), \quad (1)$$

where  $r_o(w) = r_v - \tau_o \beta(w - \bar{w})$  is the Rayleigh number at which a confined state of width  $w$  neither grows nor shrinks. Using the fit parameter  $\tau_o^{-1}$ , each measurement  $\Delta v(r, w)$  yields a value of  $r_o(w)$  which depends only weakly on the functional form assumed for the width dependence:  $r_o(w) = r - \tau_o \Delta v(r, w)$ . Figure 4 shows the dependence of this Rayleigh number on width. There appears to be a break in the slope of  $r_o(w)$  near  $w = 17$ ; since there are not enough data points at large  $w$  to determine the shape of this function there, I excluded the data point at  $w = 25.5$  from the fit in the previous paragraph and from Fig. 3. Without this point,  $r_o(w)$  is indeed an approximately linear function of width, with slope  $dr_o/dw = 4.8(3) \times 10^{-4}$  for  $7 \lesssim w \lesssim 17$ . Qualitative obser-

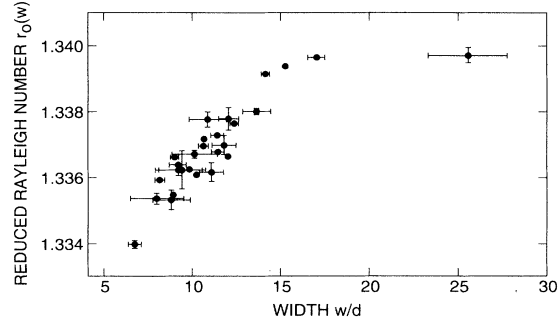


FIG. 4. Plotted as a function of the confined-state width  $w$  is the Rayleigh number  $r_o(w) = r - \tau_o \Delta v(r, w)$  at which the expansion velocity vanishes. The data for  $w \leq 17$  are well represented by a straight line of slope  $dr_o/dw = 4.8(3) \times 10^{-4}$ .  $r_o(w)$  appears to increase very weakly with  $w$  for  $w \gtrsim 20$ .

vations of very wide confined states suggest that  $dr_o/dw$  is very weakly positive for  $25 \lesssim w \lesssim 40$  [16].

The sign and magnitude of the derivative  $dr_o/dw$  are important because they determine the stability of the confined state: steady-state solutions to Eq. (1) are stable if  $dr_o/dw > 0$ . In this regime, a confined state of width  $w$  simply relaxes to the time-independent width  $w_r$  given by  $r_o(w_r) = r$ . In the present experiments, I did not wait for this to happen. If I had done so, then the data graphed in Fig. 2(b) would have exhibited a plateau at  $\Delta v = 0$ , which could have been misinterpreted as a locking band. The slight flattening of the trend of the data in the center of Fig. 2(b) is probably the effect of a partial approach to this equilibrium. Solutions of Eq. (1) for which  $dr_o/dw < 0$  are unstable. An unstable confined state will grow or shrink until it either fills the system, disappears completely, or attains a width for which  $dr_o/dw > 0$ . At  $\psi = -0.127$ , it is possible to force fixed-width TW pulses to grow into arbitrary-width confined states which are globally and strongly unstable; i.e., for which  $r_o(w)$  is a monotonically decreasing function and the expansion rate  $|\tau_o^{-1} dr_o/dw|$  is large. These unstable confined states can be maintained in a steady state only by actively controlling their width with a servo. Observations of this type will be reported in the future.

The results of these experiments are that confined states at  $\psi = -0.253$  drift backwards, do not exhibit locking, and are stable. The previous observations of stationary confined states and a rather wide locking band can undoubtedly be ascribed to pinning by inhomogeneities in the experimental cell. As in the case of fixed-width TW pulses observed at smaller  $|\psi|$ , this pinning apparently has little effect on the structure of the confined state. The observation that time-independent, “arbitrary-width” confined states actually have a unique width at a given Rayleigh number removes a long-standing discrepancy between the experimental observation of a locking band and the prediction of a discrete family of confined-state solutions for the CGLE model.

I am pleased to acknowledge continuing conversations with P. C. Hohenberg.

- [1] R. W. Walden, P. Kolodner, A. Passner, and C. M. Surko, *Phys. Lett.* **55**, 496 (1985).
- [2] In this paper, Rayleigh numbers are normalized by the critical Rayleigh number  $R_c = 1707.8$  for the onset of convection in a pure fluid in a laterally infinite geometry. These “reduced” Rayleigh numbers are written with a lower-case  $r$ .
- [3] W. van Saarloos and P. C. Hohenberg, *Physica* **D56**, 303 (1992).
- [4] E. Moses, J. Fineberg, and V. Steinberg, *Phys. Rev. A* **35**, 2757 (1987); R. Heinrichs, G. Ahlers, and D. S. Cannell, *Phys. Rev. A* **35**, 2761 (1987).
- [5] J. J. Niemela, G. Ahlers, and D. S. Cannell, *Phys. Rev. Lett.* **64**, 1365 (1990).
- [6] P. Kolodner, *Phys. Rev. A* **44**, 6448 (1991).
- [7] V. Steinberg and E. Kaplan, in *Proceedings of the NATO Advanced Research Workshop on Spontaneous Formation of Space-Time Structures and Criticality*, edited by T. Riste and D. Sherrington (Kluwer, Dordrecht, 1991), p. 207.
- [8] W. Barten, M. Lücke, and M. Kamps, *Phys. Rev. Lett.* **66**, 2621 (1991); M. Lücke, W. Barten, and M. Kamps, *Physica* **D61**, 183 (1992).
- [9] H. Riecke, *Phys. Rev. Lett.* **68**, 301 (1992); *Physica* **D61**, 253 (1992).
- [10] P. Kolodner, D. Bensimon, and C. M. Surko, *Phys. Rev. Lett.* **60**, 1723 (1988); D. Bensimon, P. Kolodner, C. M. Surko, H. Williams, and V. Croquette, *J. Fluid Mech.* **217**, 441 (1990).
- [11] C. M. Surko, D. R. Ohlsen, S. Y. Yamamoto, and P. Kolodner, *Phys. Rev. A* **43**, 7101 (1991).
- [12] D. Bensimon, B. I. Shraiman, and V. Croquette, *Phys. Rev. A* **38**, 5461 (1988).
- [13] P. Kolodner, *Phys. Rev. A* **46**, 6431 (1992).
- [14] P. Kolodner, H. Williams, and C. Moe, *J. Chem. Phys.* **88**, 6512 (1988).
- [15] The issue of the statistical vs absolute precision of the Rayleigh-number measurements in this system has been discussed in Ref. [13]. The relative uncertainty of different Rayleigh numbers measured in the same dynamical state is limited only by the stability and uniformity of the apparatus. For the spatially localized states described here, that uncertainty is given by the spatial uniformity:  $4 \times 10^{-4}$ .
- [16] The “saturated” shape of the width dependence shown in Fig. 4 has been confirmed in detail in experiments using a fluid with  $\psi = -0.210$ .